line phosphatase at this point caused high background, a sequential block with avidin and then biotin was performed first as follows: avidin (1 μM) (Pierce) was added to the TBST-G and incubated for 1 hour. Filters were then washed four times with TBST and then incubated with TBST-G and biotin (0.1 mM to 1 mM) (Sigma) for 40 min at RT with CS. Filters were washed as above and incubated with the biotinylated peptide probe (1 μg/ml) in TBST-G for 4 hours at 4°C with CS. Filters were washed as above except at 4°C then incubated for 1 hour with streptavidin alkaline phosphatase (Boehringer Mannheim) at a dilution of 1:5000 in TBST-G at 4°C with CS, washed as before, and then washed once with alkaline phosphatase buffer [100 mM tris (pH 9.5), 100 mM NaCl, and 5 mM MgCl], and developed with nitroblue tetrazolium and 5-bromo-4-chloro-3-indolyl phosphate (Promega), as described by the manufacturer.
8. Lysogens were prepared as described (*29*) except that the preparation of extracts was stopped after the lysozyme was added to thawed cell suspensions.
9. The SH3 domains of murine Src, neural Src, and the 5′ SH3 of murine Crk were prepared by reverse transcription and polymerase chain reaction (PCR) amplification of total RNA from 3T3 cells or mouse forebrain (for neural Src). Primers were synthesized with the 5′ Bam HI and 3′ Eco RI sites for insertion in-frame with the GST pGEX-2T. The Src SH3 probe contained amino acids 88 to 141 (amino acids 88 to 147 of neural Src) and did not differ from the published sequence (*18*). The Crk SH3 contained amino acids that corresponded to amino acids 372 through 428 of v-*crk* (*30*) and differs from the chicken sequence at positions corresponding to amino acids 384, 385, 396, 411, and 492, where the mouse gene encodes Glu, Glu, Arg, Ser, and Glu, respectively. These probes and a control GST probe were biotinylated (*6*).
10. Biotinylated anti–β-galactosidase antibody was purchased from Pierce.
11. The pBS vector was purchased from Stratagene.
12. Sequencing reactions were carried out with the Sequenase kit (U.S. Biochemical) according to the manufacturer's protocols.
13. E. Shtivelman, B. Lifshitz, R. P. Gale, E. Canaani, *Nature* **315**, 550 (1985).
14. C. Hall *et al.*, *J. Mol. Biol.* **211**, 11 (1990).
15. D. Diekmann *et al.*, *Nature* **351**, 400 (1991).
16. H. F. Paterson *et al.*, *J. Cell Biol.* 111, 1001 (1990).
17. Constructs 1 through 9 represent various restriction enzyme fragments of 3BP-1 subcloned from pBS in-frame with the GST of pGEX (data not shown). Constructs 10 through 12 represent 3BP-1 fragments in pGEX derived from synthetic oligonucleotide–directed PCR of the 3BP-1 cDNA. PCR fragments were constructed with synthetic oligonucleotide primers directed against internal sites in construct 9 as shown (Fig. 3A). Oligos contained 24 bp of identical sequence for hybridization and either entire Bam HI or Eco RI sites with five extra base pairs at the 5′ end for stability and recutting efficiency. The 5′ oligos were in-frame with the GST of pGEX.
18. R. Martinez, B. Mathey-Prevot, A. Bernards, D. Baltimore, *Science* **237**, 411 (1987).
19. Protein concentration of the fusion protein probes was determined with the Bio-Rad protein assay kit for standardization of the GST fusion protein probes. These proteins were further assayed by SDS-PAGE and staining with Coomassie blue. To compare the biotinylation of the protein probes, we transferred proteins in an identical gel to nitrocellulose and assayed the biotin content by binding to streptavidin alkaline phosphatase; the color was developed as described (*7*).
20. L. C. Cantley *et al.*, *Cell* **64**, 281 (1991).
21. W. S. Pear, P. Cicchetti, D. Baltimore, unpublished results.
22. R. Prywes, J. G. Foulkes, N. Rosenberg, D. Baltimore, *Cell* **34**, 569 (1983); R. Prywes, J. Hoag, N. Rosenberg, D. Baltimore, *J. Virol.* **54**, 123 (1985).
23. M. J. Fry, *Curr. Biol.* **2**, 78 (1992).
24. C. Ellis, M. Moran, F. McCormick, T. Pawson, *Nature* **343**, 377 (1990).
25. J. Settleman, V. Narasimhan, L. Foster, R. Weinberg, *Cell* **69**, 539 (1992).
26. J. Chenevert, K. Corrado, A. Bender, J. Pringle, I. Herskowitz, *Nature* **356**, 77 (1992).
27. S. G. Clark, M. J. Stern, H. R. Horvitz, *ibid.*, p. 340.
28. Y. Ben Neriah, A. Bernards, M. Paskind, G. Q. Daley, D. Baltimore, *Cell* **44**, 577 (1986).
29. R. Singh, G. Clerc, J. H. LeBowitz, *Biotechniques* **7**, 252 (1989).
30. B. J. Mayer, M. Hamaguchi, H. Hanafusa, *Nature* **332**, 272 (1988).
31. Abbreviations for the amino acid residues are: A, Ala; C, Cys; D, Asp; E, Glu; F, Phe; G, Gly; H, His; I, Ile; K, Lys; L, Leu; M, Met; N, Asn; P, Pro; Q, Gln; R, Arg; S, Ser; T, Thr; V, Val; W, Trp; and Y, Tyr.
32. The λgt11 library was the kind gift of A. Winoto. We thank P. K. Jackson for helpful discussions and the c-*abl* SH3-GST fusion probe, R. Darnell for mouse brain mRNA, A. Ray for helpful advice and the Y1089 bacterial strain, and E. Schaeffer for bacterial strain Y1090. Supported by National Research Service award training grant A107233 (P.C.), B. Duke Glenn Fellowship (P.C.), National Research Service award CA 08875 (B.J.M.), and U.S. Public Health Service grant CA 51462 (D.B.).

22 April 1992; accepted 16 June 1992

Selective Role of N-Type Calcium Channels in Neuronal Migration

Hitoshi Komuro* and Pasko Rakic

Analysis of neuronal migration in mouse cerebellar slice preparations by a laser scanning confocal microscope revealed that postmitotic granule cells initiate their migration only after the expression of N-type calcium channels on their plasmalemmal surface. Furthermore, selective blockade of these channels by addition of ω-conotoxin to the incubation medium curtailed cell movement. In contrast, inhibitors of L- and T-type calcium channels, as well as those of sodium and potassium channels, had no effect on the rate of granule cell migration. These results suggest that N-type calcium channels, which have been predominantly associated with neurotransmitter release in adult brain, also play a transient but specific developmental role in directed migration of immature neurons before the establishment of their synaptic circuits.

The majority of neurons in the developing central nervous system migrate from the site of their last cell division to their distant final positions (*1*). Proper acquisition of this position, attained through the process of active migration, ultimately affects a neuron's morphology, synaptic connectivity, and function (*2*). However, the cellular and molecular mechanisms of cell migration are not well understood. So far it has been established that in the cerebellar cortex, postmitotic granule cells migrate away from the germinal external granular layer toward the internal granular layer along the elongated fibers of Bergmann glial cells (*3*), and several cell adhesion molecules, which may play a role in this movement, have been isolated (*4*). Much less attention has been paid to the cell membrane properties and ionic concentration during cell movement. Only recently has it been recognized that migrating neurons in the developing central and peripheral nervous system express voltage-sensitive ion channels before reaching their final destinations (*5*). Here, we present evidence that the directed migration of postmitotic granule cells in the developing cerebellum requires functional ω-conotoxin–sensitive (N-type) Ca^{2+} channels.

Section of Neurobiology, Yale University School of Medicine, New Haven, CT 06510.

*To whom correspondence should be addressed.

We analyzed the mode of granule cell migration in slice preparations obtained from postnatal 10-day-old mouse cerebella labeled with a lipophilic carbocyanine dye (DiI) using a laser scanning confocal microscope. This method of analysis was chosen in preference to cultures of dissociated cells because it allows the visualization of both the soma and leading processes of migrating granule cells in situ without disturbing the ambient microenvironment (Fig. 1). The labeling of a large number of postmitotic granule cells with DiI allows precise localization of their position over time (*6*). Our measurements of the length of the migratory pathway during the first 6 hours in slice preparations indicate that the dynamics and rate of granule cell migration in vitro of 10 to 17 μm per hour are comparable to those measured in vivo (Fig. 2) (*6*). It was also possible to follow the movement of individual neurons in the slice preparation by collecting images of identified migrating granule cells every 1 to 10 min over a period of several hours. The rate of migration observed in the first 2 hours, 16.7 ± 5.0 μm per hour (mean ± SD, $n = 21$), was similar to the rate obtained from the methods described in (*6*) and is consistent with the measurements performed on cocultures of dissociated cerebellar granule and Bergmann glial cells (*7*). It also corresponds well with autoradiographic data obtained from studies of cells labeled with [^{3}H]thymidine

in intact animals (8).

After establishing that the movement of postmitotic granule cells was not adversely affected in this slice preparation for the first 6 hours, we examined whether the electrical activity of granule cells plays a significant role in their migration. Several voltage-sensitive ion currents have been observed in the immature granule cells (9), but so far have not been shown to occur during their migrating phase. Therefore, we tested several well-known ion channel blockers by adding each to the tissue culture medium in separate experiments. Blockade of the voltage-sensitive Na^+ channels by tetrodotoxin and K^+ channels by tetraethylammonium chloride or 4-aminopyridine (9) failed to alter the rate of cell migration (Fig. 3). However, the addition of Cd^{2+}, which blocks N-, L-, and T-type Ca^{2+} channels (*10*), resulted in a statistically significant slowing of cell movement ($P < 0.05$). In contrast, blocking of L- and T-type Ca^{2+} channels alone by addition of nifedipine or Ni^{2+} (*10*) had no significant effect. Finally, the addition to the medium of ω-conotoxin GVIA (ω-CgTx), an antagonist of the N-type Ca^{2+} channel (*11*), regularly curtailed granule cell migration (Fig. 3). This effect was dose-dependent in the range of 30 to 3000 nM. The smallest statistically significant decrease in the rate of neuronal migration ($P < 0.05$) was detected in a concentration of 30 nM ω-CgTx (24%), and the decrease in the rate became gradually more pronounced ($P < 0.01$) as the concentration of toxin increased: at 300 nM (50%), at 1000 nM (65%), and at 3000 nM (>78%).

Our working hypothesis is that N-type calcium channels modulate granule cell migration by controlling Ca^{2+} influx. Calcium ions have already been shown to play a role in the motility of growth cones (*12*). To test their function in migrating neurons we measured the rate of cell migration in culture medium containing Ca^{2+} above and below normal concentration of 1.8 mM. Low concentrations (0.1 to 1.0 mM) resulted in a graded significant ($P < 0.01$) decrease in the rate of migration (Fig. 4). In contrast, concentrations of 5.0 mM Ca^{2+} slightly enhanced the rate of migration, though the increment was not statistically significant (Fig. 4). These results show that the rate of cell migration is highly sensitive to fluctuations in Ca^{2+} concentration and support the hypothesis that ω-CgTx affects this rate by blocking Ca^{2+} entry into the cell.

Natural toxins such as ω-CgTx can exert specific effects only on cells that have a sufficient quantity of appropriate channels on their membranes. To determine the time of onset of expression and distribution of N-type Ca^{2+} channels on the plasmalemmal surface of granule cells, we incubated slice preparations from postnatal 10-day-old mouse cerebella with tetramethylrhodamine-conjugated ω-conotoxin (Tm-Rhd–ω-CgTx) (*13*). By confocal microscopy, we detected a striking pattern of labeling across the layers of the developing cerebellum (Fig. 5A). The outer and inner halves of the external granular layer were distinctly marked by a sharp difference in labeling. The outer half of the external granular layer, which contains mainly proliferating cells, was devoid of any fluorescence (PLZ in Fig. 5B). However, the inner half of the same layer, which is composed mainly of postmitotic cells in their premigratory phase, was clearly reactive (PMZ in Fig. 5B). The fluorescence expressed by the postmitotic granule cells was more intense during their passage through the molecular layer (ML in Fig. 5B) and attained a maximal intensity in the internal granular layer where the cells reach their final destination (GL in Fig. 5A). Therefore, N-type Ca^{2+} channels are present at the appropriate time and place on the immature granule cell surface and could easily be bound by ω-CgTx during their migration.

Our results suggest that the activity of voltage-sensitive N-type Ca^{2+} channels is crucial to granule cell migration. In contrast, the activity of voltage-sensitive Na^+, K^+, and L- and T-type Ca^{2+} channels seems to be far less or not significant for migration. This finding is surprising because N-type Ca^{2+} channels are not known to modulate cytoskeletal and contractile proteins but rather have been mainly implicated in the release of neurotransmitters (*11*). Furthermore, growth cone movement (*14*), neurite extension (*15*), and neural crest cell migration (*5*) in cell cultures appear to be regulated, for the most part, by the activity of L-type Ca^{2+} channels. At present, we do not know the amount and subtype distribution of Ca^{2+} channels on the plasmalemmal surface of migrating neurons. The ratio of N-type to L-type channels varies considerably between in vitro and in vivo environments, between cell classes, and between developing and adult tissues (*16*). Furthermore, N-type Ca^{2+} channels are a quite heterogeneous group (*11*). It is therefore possible that during the migration phase immature granule cells possess different subtypes and ratios of Ca^{2+} channels than after arrival at their final destination

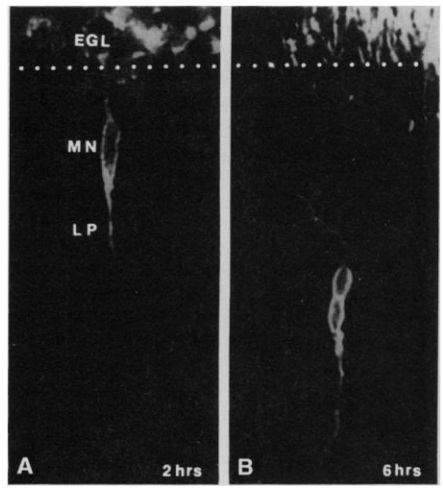

Fig. 1. Migrating granule cells in the slice preparation (**A**) 2 and (**B**) 6 hours after staining with carbocyanine dye (DiI). The soma of a migrating neuron (MN) as well as its leading process (LP) could be identified. The border between the external granule layer (EGL) and molecular layer is marked by a dotted line. In these experiments, 10-day-old mouse cerebella were sectioned sagittally into 800-μm-thick slices and stained for 30 min with DiI (10 μg/ml, Molecular Probes, Eugene, OR) added to a cell culture medium. The incubation medium consisted of minimum essential medium (MEM) (Gibco) supplemented with 40 mM glucose, 1.8 mM glutamine, 24 mM $NaHCO_3$, penicillin (90 U/ml), and streptomycin (90 μg/ml). After staining for 30 min at 37°C, preparations were rinsed with plain incubation medium and maintained in an incubator (37°C, 95% air, 5% CO_2). At 2, 4, and 6 hours several slice preparations were fixed with 10% formalin in 0.1 M phosphate buffer (pH 7.4) and cut into sections 200 μm thick in the sagittal plane. Only sections obtained from the middle of the slice were used for quantitative analysis.

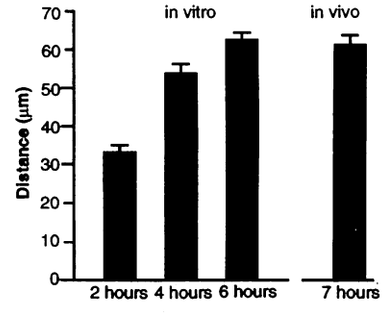

Fig. 2. The relation between the mean distance traversed by labeled granule cells and the time elapsed between the end of staining with DiI and fixation. All three sets of in vitro experiments were conducted on cerebellar slices obtained from 10-day-old mice. Each column is an average of at least 100 neurons. Bar, SEM. The distance attained by neurons at different time points differed statistically ($P < 0.01$). For the in vivo experiments, 10-day-old mice were anesthetized, a hole was bored in each of their skulls, and a tiny crystal of DiI was placed on the exposed cerebellar external granular layer. Cerebella were fixed 7 hours later by exposure to 10% formalin in 0.1 M phosphate buffer (pH 7.4) and sectioned sagittally into 200-μm-thick sections. The mean migrating distance obtained from in vivo experiments is comparable to the distance obtained from in vitro analyses.

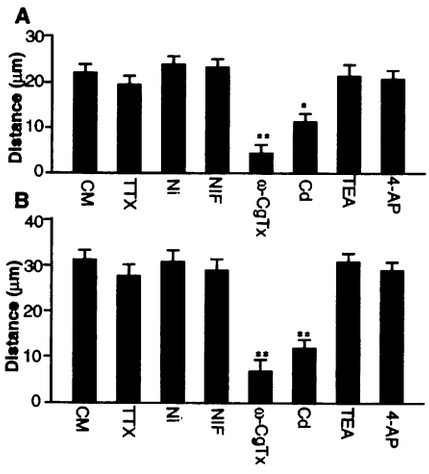

Fig. 3. The effect of several ion channel blockers on granule cell migration in cerebellar slice preparations. All preparations were obtained from 10-day-old mice. Each bar is an average of at least 100 cells. Small bar, SEM. Before the addition of various ion channel blockers, the granule cells were labeled with DiI and the slice preparations were maintained in culture medium for 2 hours as described in Fig. 1. Subsequently, specific Ca^{2+}, Na^+, and K^+ channel blockers were added and preparations maintained for an additional (**A**) 2 to (**B**) 4 hours. At either time, the mean distance of cell displacement in control slice preparations (CM) was not significantly different from the values obtained after the addition of 10 μM tetrodotoxin (TTX), which blocks Na^+ channels, 100 μM Ni^{2+} (Ni), which blocks T-type Ca^{2+} channels, 5 μM nifedipine (NIF), which blocks L-type Ca channels, and 20 μM tetraethylammonium (TEA) or 2 μM 4-aminopyridine (4-AP), which blocks K^+ channels. However, addition of 3 μM ω-conotoxin (ω-CgTx) and 100 μM Cd^{2+} (Cd), which block the N-type and all types of Ca^{2+} channels, respectively, reliably inhibited cell movement. We obtained each mean migratory distance by subtracting the mean displacement of the cell soma at 2 hours in culture (Fig. 2) from the total length of the migratory pathway. Single ($P < 0.05$) and double ($P < 0.01$) asterisks indicate statistical significance.

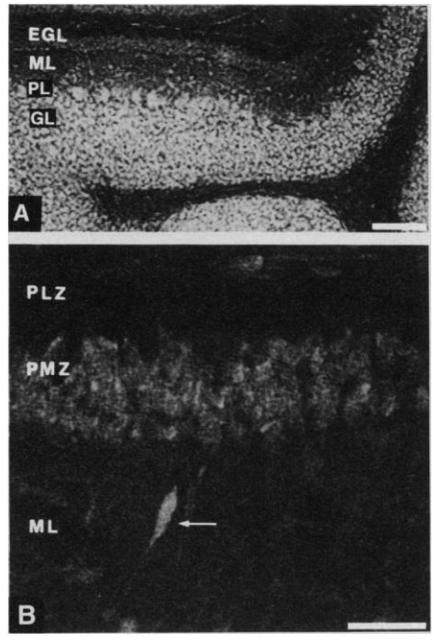

Fig. 5. Distribution of ω-CgTx–sensitive Ca^{2+} channels in the cerebellum of 10-day-old mice. Slice preparations cut sagittally at about 300 μm were incubated with 1 μM tetramethylrhodamine-conjugated ω-CgTx (TmRhd–ω-CgTx, List Biological, Campbell, California) in MEM for 60 min at room temperature and rinsed with the same culture medium for an additional 2 hours. The binding sites of TmRhd–ω-CgTx were visualized with a confocal microscope. (**A**) Low-power overview of the developing cerebellum, which shows gradual increase in staining density from the external granular layer (EGL) across the molecular layer (ML) to the Purkinje cell layer (PL) and internal granular layer (GL). Scale bar, 100 μm. (**B**) Higher power microphotograph displays absence of fluorescence in the outer proliferative zone (PLZ) and moderate staining in the inner premigratory zone (PMZ) of the external granular layer. Bipolar migrating cell (arrow), which moves across the molecular layer, is well-distinguished by fluorescence of the soma and leading process. Scale bar, 25 μm.

in the internal granular layer.

At present, there is no direct evidence that migrating granule cells generate the spontaneous electrical activity or elevation of intracellular Ca^{2+} concentrations by the activation of N-type Ca^{2+} channels. However, in tissue culture experiments immature granule cells generate spontaneous electrical activity (*17*) and show elevations of intracellular Ca^{2+} after the application of glutamate to the medium (*18*). Furthermore, undifferentiated spinal neurons exhibit spontaneous elevation of intracellular Ca^{2+} (*19*). This transient elevation of intracellular Ca^{2+} was inhibited by application of 5 μM ω-CgTx to the medium (*19*). Therefore, the activation of N-type Ca^{2+} channels can cause elevation of intracellular Ca^{2+} in migrating granule cells, although these channels may not behave as "classical" N-type channels (*20, 21*).

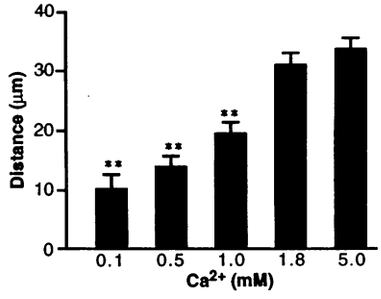

Fig. 4. The effect of various concentrations of Ca^{2+} in tissue culture medium on the rate of granule cell migration. All preparations were obtained from 10-day-old mice. Each bar is an average of at least 100 cells. Small bar, SEM. After labeling the slice preparations with DiI, we maintained them in control culture medium (1.8 mM Ca^{2+}) for 2 hours. Subsequently, the control culture medium was changed to low or high Ca^{2+} culture medium and preparations were maintained for an additional 4 hours. We obtained each mean migratory distance by subtracting the mean displacement of the cell soma at 2 hours in culture (Fig. 2) from total length of the migratory pathway. Double asterisks indicate statistical significance at the $P < 0.01$ level.

Calcium ion channels are thought to control Ca^{2+} influx, which in turn influences a variety of important cellular functions ranging from membrane excitability and neurotransmitter secretion to differential gene expression (*22*). Our results suggest that Ca^{2+} influx through N-type Ca^{2+} channels is also essential for directed neuronal migration. However, unlike surface molecules that are thought to be involved in the recognition of migratory pathways and adhesion between neurons and glial cells (*1, 4*), N-type Ca^{2+} channels probably play a permissive role in neuronal migration. For example, activation of voltage-sensitive Ca^{2+} channels on neural crest cells changes cytosolic free Ca^{2+} concentrations and thereby can influence both the onset of cell migration and the degree of cell-cell adhesion (*23*). Furthermore, Ca^{2+} is involved in cytoskeletal formation and the activity of actin-binding contractile proteins (*12*) and thereby may be necessary for proper motility of the leading process of the cell or translocation of its nucleus (*1*). It is also possible that Ca^{2+} regulation is linked to changes in adhesion molecules such as neural cell adhesion molecules and N-cadherin, which participate in morphological differentiation (*24*). Because migrating granule cells express several cell adhesion molecules (*4*), some of these molecules might regulate and activate N-type Ca^{2+} channels (*24*). Therefore, the early expression of ω-CgTx–sensitive Ca^{2+} channels in postmitotic cells may be an essential prerequisite to both the initiation and the execution of their movement.

REFERENCES AND NOTES

1. P. Rakic, in *The Cell in Contact*, G. M. Edelman and J.-P. Thiery, Eds. (Wiley, New York, 1985), pp. 67–91; *Experientia* **46**, 882 (1990).
2. V. S. Caviness, Jr., and P. Rakic, *Annu. Rev. Neurosci.* **1**, 297 (1978); P. Rakic, *Prog. Brain Res.* **73**, 15 (1988).
3. P. Rakic, *J. Comp. Neurol.* **141**, 283 (1971); *Brain Res.* **33**, 471 (1971).
4. C.-M. Choung, K. L. Crossin, G. M. Edelman, *J.*

Cell Biol. **104**, 331 (1987); J. C. Edmonson, R. K. H. Liem, J. E. Kuster, M. E. Hatten, *ibid.* **106**, 505 (1988); H. Antonicek and M. Schachner, *J. Neurosci.* **8**, 2961 (1988); C.-M. Chuong, *Experientia* **46**, 892 (1990).
5. J. J. LoTurco, M. G. Blanton, A. R. Kriegestein, *J. Neurosci.* **11**, 792 (1991); D. Moran, *Am. J. Anat.* **192**, 14 (1991).
6. Using a serial assay technique, we estimated the average length of the migratory pathway in vitro by measuring the distance from the DiI-labeled cell soma to the border between the external granular and the molecular layers at different time points (Fig. 1). The mean length of the migration route for labeled cells after 2 hours was 33.0 ± 15.9 μm (mean ± SD, n = 151), a rate of 16.5 μm per hour (Fig. 2). The migrating route was 53.5 ± 22.7 μm (n = 136) after 4 hours and 62.5 ± 22.1 μm (n = 136) after 6 hours, which indicated that the speed of migration slows down with time (Fig. 2). To determine whether these measurements reflect granule cell migration in vivo, we next stained migrating granule cells in living animals by applying DiI on the cerebellar surface and then examined their position in fixed tissue with confocal microscopy (MRC-600, Bio-Rad). The mean displacement of granule cells in vivo was 61.2 ± 25.2 μm per 7 hours (n = 122), a distance comparable to that obtained in slice preparations (Fig. 2).
7. G. Fishell and M. E. Hatten, *Development* **113**, 755 (1991).
8. S. Fujita, *J. Cell Biol.* **32**, 277 (1967).
9. S. B. Cull-Candy, C. G. Marshall, D. Ogden, *J. Physiol. (London)* **414**, 179 (1989); P. A. Slesinger and J. B. Lansman, *ibid.* **435**, 101 (1991); C. Marchetti, C. Carignani, M. Robello, *Neuroscience* **43**, 121 (1991).
10. R. W. Tsien *et al.*, *Trends Neurosci.* **11**, 431 (1988).
11. P. Hess, *Annu. Rev. Neurosci.* **13**, 337 (1990); E. Sher and F. Clementi, *Neuroscience* **42**, 301 (1991); W. A. Horne, E. Hawrot, R. W. Tsien, *J. Biol. Chem.* **266**, 13719 (1991); B. M. Olivera, J. Rivier, J. K. Scott, D. R. Hillyard, L. J. Cruz, *ibid.*, p. 22067.
12. P. Forscher, *Trends Neurosci.* **12**, 468 (1989).
13. O. T. Jones, D. L. Kunze, K. J. Angelides, *Science* **244**, 1189 (1989).
14. S. B. Kater and L. R. Mills, *J. Neurosci.* **11**, 891 (1991).
15. S. J. Robson and R. D. Burgoyne, *Neurosci. Lett.* **104**, 110 (1989).
16. J. A. Wagner *et al.*, *J. Neurosci.* **8**, 3354 (1988); N. Martin-Moutot, M. Seagar, F. Couraud, *Neurosci. Lett.* **115**, 300 (1990); A. Vigers and K. H. Pfenninger, *Dev. Brain Res.* **60**, 197 (1991).
17. P. E. Hockberger, H.-Y. Tseng, J. A. Connor, *J. Neurosci.* **7**, 1370 (1987).
18. J. A. Connor, H.-Y. Tseng, P. E. Hockberger, *ibid.*, p. 1384; M. J. Courtney, J. J. Lambert, D. G. Nicholls, *ibid.* **10**, 3873 (1990).
19. J. Holliday and N. C. Spitzer, *Dev. Biol.* **141**, 13 (1990).
20. M. C. Nowycky, A. P. Fox, R. W. Tsien, *Nature* **316**, 440 (1985).
21. C. R. Artalejo, R. L. Perlman, A. P. Fox, *Neuron* **8**, 85 (1992).
22. R. J. Miller, *Science* **235**, 46 (1987).
23. D. F. Newgreen and D. Gooday, *Cell Tissue Res.* **329**, 329 (1985).
24. P. Doherty, S. V. Ashton, S. E. Moore, F. S. Walsh, *Cell* **67**, 21 (1991).
25. This research was supported by the U.S. Public Health Service and by a Human Frontiers grant from Japan. We thank R. Cameron, P. S. Goldman-Rakic, and K. Wikler for useful suggestions and comments on the manuscript.

30 March 1992; accepted 17 June 1992

Interferon-Dependent Tyrosine Phosphorylation of a Latent Cytoplasmic Transcription Factor

Chris Schindler, Ke Shuai, Vincent R. Prezioso, James E. Darnell, Jr.*

The interferon-α (IFN-α)–stimulated gene factor 3 (ISGF3), a transcriptional activator, contains three proteins, termed ISGF3α proteins, that reside in the cell cytoplasm until they are activated in response to IFN-α. Treatment of cells with IFN-α caused these three proteins to be phosphorylated on tyrosine and to translocate to the cell nucleus where they stimulate transcription through binding to IFN-α–stimulated response elements in DNA. IFN-γ, which activates transcription through a different receptor and different DNA binding sites, also caused tyrosine phosphorylation of one of these proteins. The ISGF3α proteins may be substrates for one or more kinases activated by ligand binding to the cell surface and may link occupation of a specific polypeptide receptor with activation of transcription of a set of specific genes.

Many polypeptide growth factors and cytokines induce the transcription of largely nonoverlapping sets of genes (*1–5*). The basis for this high degree of specificity in gene activation by particular polypeptide ligands is not known. Many cell surface receptors have intrinsic biochemical activities that transmit signals to the cell interior (*6–8*). For example the internal domains of the receptors for platelet-derived growth factor and epidermal growth factor (*6*, *8*) have tyrosine kinase activity that is required for their biologic function. However, the receptors for many ligands such as growth hormone, tumor necrosis factor, interleukin-1, IFN-α, and IFN-γ do not have known enzyme activities associated with them (*1–5*). However some of these receptors could have associated kinases such as $p56^{lck}$, which associates with the CD4 portion of the T cell receptor complex (*9*). A number of tyrosine kinase substrates, particularly serine threonine kinases, are targets of cell surface–associated enzymes (*10–13*). However, no substrate has been described that serves to link tyrosine kinase activity at the cell surface to stimulation of transcription in the nucleus (*14*).

We have studied genes whose transcription is stimulated by binding of IFN-α and IFN-γ to their specific cell surface receptors (*1*, *15*, *16*). In the case of IFN-α, the factor responsible for the transcriptional activation is a complex of four proteins termed ISGF3 (interferon-stimulated gene factor 3) (*17–19*). Three of these proteins, collectively termed ISGF3α proteins, reside in the cytoplasm in unstimulated cells (*18*). In cells stimulated with IFN-α, these proteins, which are 113, 91, and 84 kD in size (*19*), are translocated to the nucleus where, together with a 48-kD DNA binding protein (*19*, *20*), they form the ISGF3 complex. ISGF3 binds tightly to a specific DNA sequence, the ISRE, or interferon stimulated response element (*17*, *21*) and directs IFN-α–dependent gene transcription in the nucleus. We have cloned cDNAs that encode the 48-kD DNA binding protein (*22*) and the 113-, 91-, and 84-kD ISGF3α proteins (*23*, *24*) and prepared several different antisera to portions of these proteins.

The NH_2-terminal 701 amino acids of the 91- and 84-kD proteins are identical, and the 91-kD protein contains 38 additional amino acids at its COOH-terminus (*23*). The 113-kD protein is a member of the same gene family as the 91- and 84-kD proteins and shares about 40% amino acid identity with the 91- and 84-kD proteins, but can be distinguished by specific antisera (*24*). Three rabbit antisera were prepared to bacterial fusion proteins and used to examine IFN-induced changes in the abundance of the proteins: antiserum to amino acids 671 to 806 of the 113-kD protein (anti-113), antiserum to amino acids 598 to 705 of the 91-kD protein (anti-91), and antiserum to the COOH-terminal 36 amino acids of the 91-kD protein (anti-91T). Protein extracts from untreated [^{35}S]methionine-labeled cells were used to test each antiserum. Anti-113 precipitated only the 113-kD protein (Fig. 1A). Anti-91 precipitated both the 91- and 84-kD proteins (Fig. 1B) and anti-91T precipitated only the 91-kD protein (Fig. 1B). Thus, in untreated cells the three proteins appear not to be associated with one another.

Extracts of HeLa cells treated with IFN-α, IFN-γ alone, or IFN-α after prior treatment with IFN-γ were examined. IFN-α alone activates ISGF3, but IFN-γ alone does not (*18*, *19*). However, treatment of HeLa cells with IFN-γ for 16 to 18 hours renders them ten times more responsive to IFN-α than untreated cells and ten times more ISGF3 is formed (*25*). This enhanced response of HeLa cells is due at least in part to an increased amount of the

Laboratory of Molecular Cell Biology, The Rockefeller University, New York, NY 10021.

*To whom correspondence should be addressed.